

# Adsorption of carbon disulfide on activated carbon modified by Cu and cobalt sulfonated phthalocyanine

Fei Wang<sup>1</sup> · Xueqian Wang<sup>1</sup> · Ping Ning<sup>1</sup> · Xuli Jing<sup>1</sup> · Yixing Ma<sup>1</sup> ·  
Ping Wang<sup>1</sup> · Wei Chen<sup>1</sup>

Received: 22 March 2015 / Revised: 2 June 2015 / Accepted: 23 June 2015 / Published online: 3 July 2015  
© Springer Science+Business Media New York 2015

**Abstract** A series of adsorbents were studied for removal efficiency of carbon disulfide ( $\text{CS}_2$ ) under micro-oxygen conditions. It was found that activated carbon modified by Cu and cobalt sulfonated phthalocyanine (CoSPc) denoted as ACCu–CoSPc showed significantly enhanced adsorption ability. Reaction temperature was found to be a key factor for adsorption, and 20 °C seems to be optimal for  $\text{CS}_2$  removal. Samples were analyzed by  $\text{N}_2$ -BET, XRD, XPS, SEM–EDS and  $\text{CO}_2$ -TPD. The characterization results demonstrated that large quantities of  $\text{SO}_4^{2-}$  anions were formed and adsorbed in the reaction process.  $\text{SO}_2$ ,  $\text{CS}_2$  and COS were detected in the effluent gas generated from the temperature programmed desorption of ACCu–CoSPc– $\text{CS}_2$ . Therefore, it can be concluded that ACCu–CoSPc most likely acted as a catalyst in the adsorption/oxidation process on the surface of the impregnated sample. The generated sulfide and sulfur oxide can cover the active sites of adsorbents, resulting in pronounced reduction of adsorbent activity. Finally, the exhausted ACCu–CoSPc can be regenerated by thermal desorption.

**Keywords**  $\text{CS}_2$  adsorption · Activated carbon · Impregnation · Regeneration

## 1 Introduction

Carbon disulfide ( $\text{CS}_2$ ) is a type of the sulfur-containing compounds existing in natural gas, petroleum gas, water gas and typical industrial tail gas (Williams et al. 1999). A small amount of  $\text{CS}_2$  emission is inadmissible, since it is high toxicity with a maximum permissible concentration in air of 0.5 mg/m<sup>3</sup> (Yang et al. 2006). The presence of feedstock  $\text{CS}_2$  can also lead to increased corrosion of the reactors used in refinery processes (Ghittori et al. 1998), which triggers an increasing interest in finding reliable technologies for its control. Several methods have been developed for  $\text{CS}_2$  removal, including catalyzed—hydrolysis, catalyzed—hydrogenation, catalyzed—oxidation adsorption, etc.

Alternative proposals include hydrolysis oxidation and hydrogenation. Hydrolysis is a viable approach for  $\text{CS}_2$  removal (Tong et al. 1992; Zhao et al. 2003; Wang et al. 2013),  $\text{CS}_2$  can be efficiently converted to COS and  $\text{H}_2\text{S}$  at 300 °C or higher in the presence of water. With the method of oxidation,  $\text{CS}_2$  can be converted to S. Hydrogenation based on the formation of  $\text{H}_2\text{S}$  (Allali et al. 1995). However, the rigorous reaction conditions, including high temperature, high pressure and the existence of extraneous components, hindered its practical application.

Until now, most studies focus on reaction conditions in excess of 200 °C (Wang et al. 2007), and only a few examples were reported to operate at a temperature below 100 °C. Studies aiming to remove  $\text{CS}_2$  at low temperature (below 100 °C) are of special interests, because they can be extremely cost-effective and possess remarkable industrial applicability.

Due to its stable structure, large specific surface area, well-developed porous structure, activated carbon (AC) has found broad applications in various fields (Planeix et al. 1994; Brasquet and Le Cloirec 1997) including catalyst

✉ Xueqian Wang  
wxqian3000@aliyun.com

Ping Ning  
ningping58@sina.com

<sup>1</sup> Faculty of Environmental Science and Engineering, Kunming University of Science and Technology, Kunming 650500, China

support, development of adsorbent and conductive materials. Recent research on AC has been centered on novel modification and characterization, which could certainly help to meet the growing demand of clean air. Transition metals such as Cu have been explored in adsorption and oxidation processes. Ning et al. (2011) reported that  $\text{Cu}(\text{CH}_3\text{COO})_2$  can be used to modify AC for the adsorption of  $\text{CS}_2$ ,  $\text{H}_2\text{S}$ , COS, and  $\text{PH}_3$ , and the resulting material exhibited adsorption and oxidation properties significantly improved. In this work, Cu is chosen as the active ingredient. Mei et al. reported that  $\text{NiO}/\text{MgO}/\text{Al}_2\text{O}_3$ –CoPcS can be used for mercaptan oxidation, in which CoPcS (sulfonated cobalt phthalocyanine) could create additional oxidation sites (Mei et al. 2007).

Adsorbents were prepared by using an impregnation method (Bandosz 1999; Bandosz 2002), and the effects of experimental conditions such as the types of impregnant, reacting temperature have been explored, so as to obtain “optimal” adsorption purification conditions for  $\text{CS}_2$ . Subsequently, the adsorption mechanism involved in the adsorption purification was further clarified. The adsorbent samples prepared in our laboratory were characterized by different techniques including BET, XRD, XPS, SEM–EDS and  $\text{CO}_2$ -TPD.

## 2 Materials and methods

### 2.1 Adsorbent preparation

All adsorbents have been prepared by impregnation method. AC prepared from commercial coal-derived carbon (Jiulong Fine Chemical Factory, Chongqing, China) was used as an adsorbent support in the experiments.  $\text{Cu}(\text{NO}_3)_2 \cdot 3\text{H}_2\text{O}$ ,  $\text{Fe}(\text{NO}_3)_3 \cdot 9\text{H}_2\text{O}$ ,  $\text{Ni}(\text{NO}_3)_2 \cdot 6\text{H}_2\text{O}$ , and cobalt sulfonated phthalocyanine (CoPcS) were used as impregnants in order to improve the adsorption performance of the AC. To remove soluble impurities, each support ( $10 \pm 0.1$  g) was washed with 150 mL of distilled water at 70 °C for three times, and then dried 110 °C for 12 h (denoted AC). Subsequently, AC samples were impregnated with an aqueous  $\text{Cu}(\text{NO}_3)_2$  solution (0.15 mol/L, 50 mL), an aqueous  $\text{Fe}(\text{NO}_3)_3$  solution (0.15 mol/L, 50 mL), an aqueous  $\text{Ni}(\text{NO}_3)_2$  solution (0.15 mol/L, 50 mL), or the combination of  $\text{Cu}(\text{NO}_3)_2$  solution (0.15 mol/L, 50 mL) and CoPc solution (0.1 g/gAC, 50 mL). The impregnation was carried out under stirring for 24 h, and then the reaction solution was filtered to give the adsorbent, which was dried at 110 °C for 12 h, followed by calcination at a specific temperature (250–400 °C) in a muffle furnace under the pressure of 82.5 kPa in air. Samples impregnated with different metals were denoted as ACCu, ACFe, ACNi and ACCu–CoPc, respectively.

### 2.2 Characterization

Multi-spot nitrogen adsorption meter NOVA2000e (Quantachrome Corp.) was used to determine nitrogen adsorption isotherms at 77.35 K. Temperature programmed desorption (TPD) experiments were performed after  $\text{CO}_2$  adsorption on samples. The desorption kinetics and products can be determined by  $\text{CO}_2$ -TPD. The exiting gas was subject to sulfur analysis by an online HC-6 sulfur phosphorus microscale analyzer with a SF-1 packed column (GDX-104 monomer) and a FPD detector. XRD analysis was conducted on a Rigaku diffraction meter (D/MAX-2200), which was operated under the conditions of 36 kV and 30 mA using Ni filtered  $\text{Cu K}\alpha$  radiation ( $\lambda = 0.15406$  nm) at a rate of 4°/min from  $2\theta = 5$ –90°. Moreover, powdered samples were directly analyzed without pre-treatment. Crystalline phase was identified by matching with Joint Committee on Powder Diffraction Standards (JCPDS) files. XL30ESEM-TMP environmental scanning electron microscope produced by PHILIPS-FEI Company, and EDAX spectrum analyzer from Phoenix were used in this work. X-ray photoelectron spectroscopy (XPS) analysis was carried out on a Physical Electronics PHI5600 spectrometer, in which the X-ray source was operated with an  $\text{Al K}\alpha$  anode at photo-energy of  $h\nu$  1 keV. The core level binding energy of C 1s for carbon at 284.8 eV was used as the internal reference for calibration.

### 2.3 Experimental procedure

The capacities of the adsorbents were measured with model gas which was composed of nitrogen with 1100 mg/m<sup>3</sup>  $\text{CS}_2$ . The model gas mixed evenly with micro-oxygen in the mixer and introduced into the adsorption bed unit. In this work, we developed an effective method to remove  $\text{CS}_2$  gas utilizing modified AC at low temperature (<100 °C) with a gas hourly space velocity (GHSV) of 1500/h.

The breakthrough point (10 %) of  $\text{CS}_2$  is determined by analyzing the inlet and outlet concentration of  $\text{CS}_2$ :

$$\text{CS}_2 \text{ breakthrough point (10\%)} = \text{CS}_2 \text{ outlet/CS}_2 \text{ inlet}$$

## 3 Results and discussion

### 3.1 Effects of modifiers on $\text{CS}_2$ adsorption

Five adsorbents modified with different impregnants, denoted as AC, ACCu, ACFe, ACNi, ACCu–CoPc, were studied and their adsorption capacities were measured and compared in dynamic removal capacity tests of  $\text{CS}_2$ . The breakthrough curves of the above adsorbents are plotted in

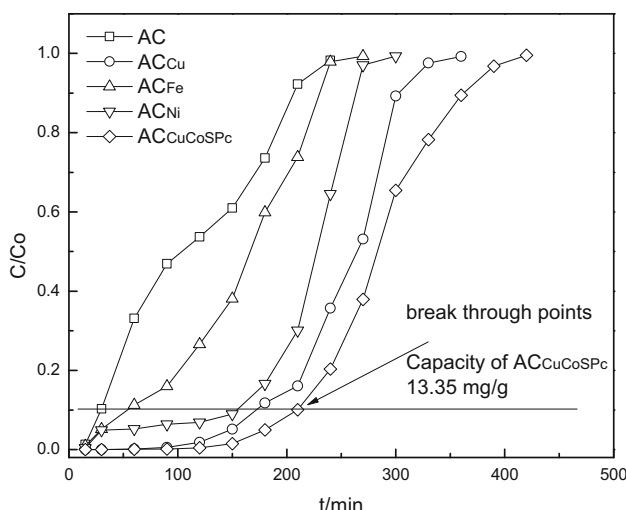


**Fig. 1**  $\text{CS}_2$  adsorption curves on different adsorbents at 40 °C in the presence of 1.0 %  $\text{O}_2$  ( $\text{CS}_2$  inlet concentration 1027 mg/m<sup>3</sup>)

Fig. 1. Their breakthrough curves differ from their performance as  $\text{CS}_2$  adsorbents, which clearly show the efficiency of the treatment for the  $\text{CS}_2$  removal. Compared with AC, ACFe, and ACNi, sample ACCu displayed a significant improvement on  $\text{CS}_2$  adsorption. What's more, it can be seen that the ability of  $\text{CS}_2$  adsorption displayed a further improvement after the addition of CoSPc, as demonstrated by a breakthrough time of 210 min and  $\text{CS}_2$  adsorption capacity of 13.35 mg  $\text{CS}_2/\text{g}$  AC. This might because CoSPc can increase the oxidation function of adsorbent. Thus, parts of the  $\text{CS}_2$  were removed through the oxidation process and the removal efficiency of ACCu–CoSPc was improved.

### 3.2 Effects of CoSPc concentration in impregnation solutions

The influence of CoSPc concentration on breakthrough curve of  $\text{CS}_2$  was studied. As is shown in Fig. 2, With the CoSPc concentration increase, the purification capacity of ACCu–CoSPc experienced the growth process after a decline. The  $\text{CS}_2$  removal efficiency range as follows: 1.0 > 2.0 > 0.5 > 1.5 > 2.5 (g/L). To some extent, the increase of CoSPc concentration may improve the loading capacity on the Cu-based AC and shorten the distance of  $\text{Co}^{2+}$ – $\text{Co}^{3+}$  centers which work as oxidation, improved their performance for the purification of  $\text{CS}_2$ . However, the activity of ACCu–CoSPc decreased when the CoSPc concentration was above 1.0 g/L. This probably because the excessive load resulted in the aggregation of the CoSPc molecules (Liu et al. 2000). There may still generate peroxide dimer  $-\text{Co}(\text{III})-\text{O}-\text{O}-\text{Co}(\text{III})-$ , which material has less activity, cover the surface of modified carbon and

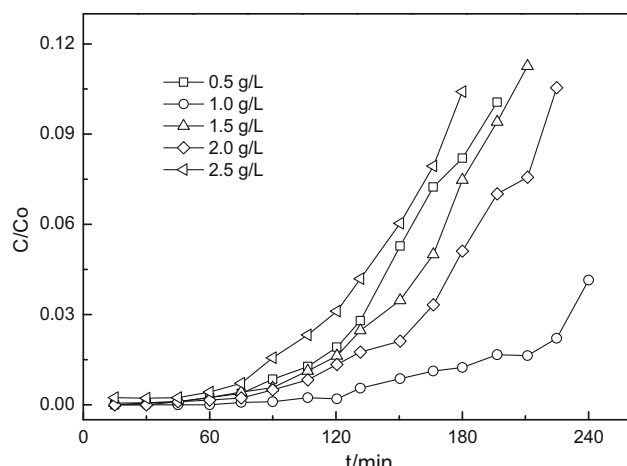


**Fig. 2** Influence of CoSPc concentration in adsorbent on breakthrough curve of  $\text{CS}_2$

blocked some of the pores. In this case, the diffusion resistance will be increased in the gas–solid phase system, which will reduce the contact and reaction opportunities between  $\text{CS}_2$  and active sites.

### 3.3 Effects of reaction temperature

Temperature is also an important factor in the gas–solid phase adsorption reaction, which has been closely examined in this paper as well. Figure 3 shows the outlet  $\text{CS}_2$  over the time as a function of temperatures at 20, 40, 60 and 80 °C. Notably, it was found that reaction temperature is one of the most critical factors that can affect the  $\text{CS}_2$  removal efficiency of. When temperature was increased from 20 to 80 °C, the breakthrough time for  $\text{CS}_2$  declined

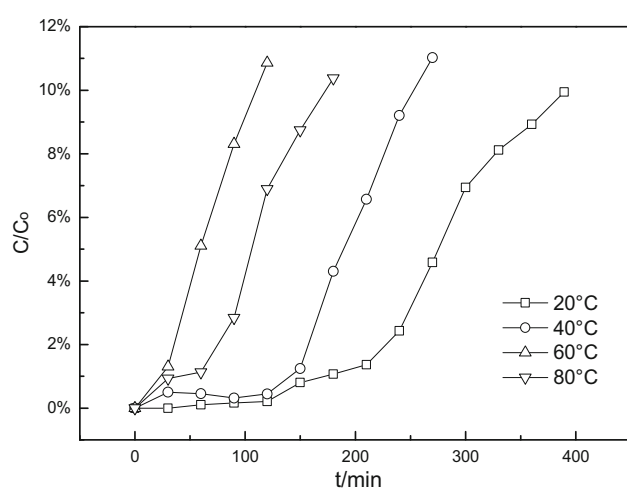


**Fig. 3** Influence of reaction temperature on breakthrough curve of ACCu–CoSPc in the presence of 1.0 %  $\text{O}_2$  ( $\text{CS}_2$  inlet concentration is 1027 mg/m<sup>3</sup>)

from 6 to 2 h, indicating that the removal efficiency of ACCu–CoSPc has been substantially reduced. As we know, adsorption process is exothermic, thus a lower temperature should favor the purification of  $\text{CS}_2$ . However, further analyses of XPS and TPD demonstrated that some quantities of  $\text{SO}_4^{2-}$  anions as well as  $\text{SO}_2$ ,  $\text{CS}_2$  and  $\text{COS}$  were formed during the reaction process. That is to say, the removal process was not a sole physical adsorption process. Actually, both physical and chemical adsorption seems to be involved in the  $\text{CS}_2$  adsorption process. Therefore, it can be concluded that the “optimal” reaction temperature for ACCu–CoSPc is 20 °C, at which the  $\text{CS}_2$  adsorption capacity was found to be 72.46 mg  $\text{CS}_2$ /g AC.

### 3.4 $\text{N}_2$ adsorption/desorption of ACCu–CoSPc

The nitrogen adsorption isotherms of ACraw/ACCu–CoSPc, catalysts was studied, and the results were shown in Fig. 4. Pore size distributions of the catalysts prepared were plotted in Fig. 5. The BET surface area, average pore radius, micro and total pore volume of samples were summarized in Table 1.

Based on the guidelines reported for BDDT classification, all nitrogen adsorption–desorption isotherms belong to the BDDT type I (Brunauer et al. 1940) classification, which is typical microporous material. Notably, the limiting uptake of such material should be governed by the accessible micropore volume, rather than the internal surface area. As illustrated in Fig. 4, the  $\text{N}_2$  adsorption capacity of plain AC seems to be greater than ACCu–CoSPc, which was probably due to the fact that pores are partially covered by the active ingredient loaded, resulting in the decline of surface area.

As shown in Fig. 5, it appears that most pore volumes are below 2 nm. The pore size distributions were

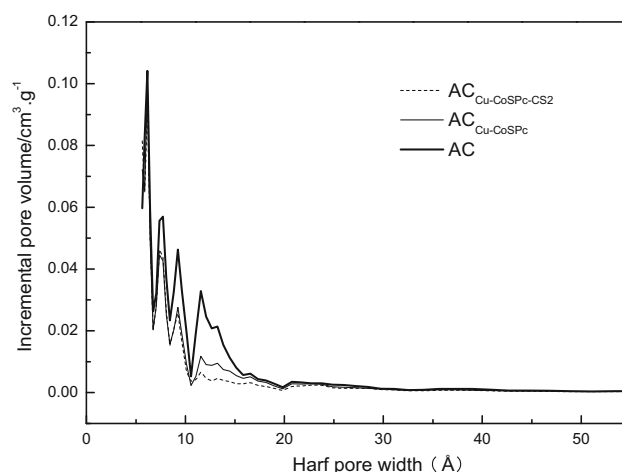


**Fig. 5** Pore size distribution of different samples

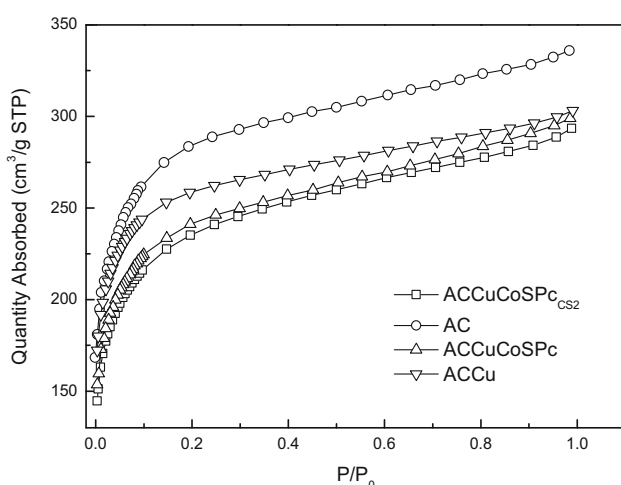
determined by density function theory (DFT) (Oliver et al. 2005; Cui and Turn 2009). Notably, the volume of micropores smaller than 2 nm was found to decrease after modification with Cu–CoSPc and the most noticeable change comes from 0.7 to 1.5 nm. Of particular interest, the volume of micropores ranges in the order of  $\text{AC} > \text{ACCu–CoSPc} > \text{ACCu–CoSPc–CS}_2$ . This phenomenon might result from the fact that pores were blocked by active ingredients and further exposure to  $\text{CS}_2$  results a more visible decrease of micropore volume.

As shown in Table 1, both surface area and volume seem to decrease after modification. Compared with AC, the surface area of ACCu–CoSPc and ACCu–CoSPc–CS<sub>2</sub> were reduced to 19.05 and 25.61 %, respectively. The volume of the micropores decreased by 13.83 and 28.51 %, respectively.

Figures 4, 5 and Table 1 show the comparison between ACCu–CoSPc and ACCu–CoSPc–CS<sub>2</sub>. Significant changes are observed in the adsorbent because of the adsorption of  $\text{CS}_2$ . Thus, the activated ingredients Cu–CoSPc loaded in micropores played an important role in  $\text{CS}_2$  adsorption.

### 3.5 SEM–EDS analysis

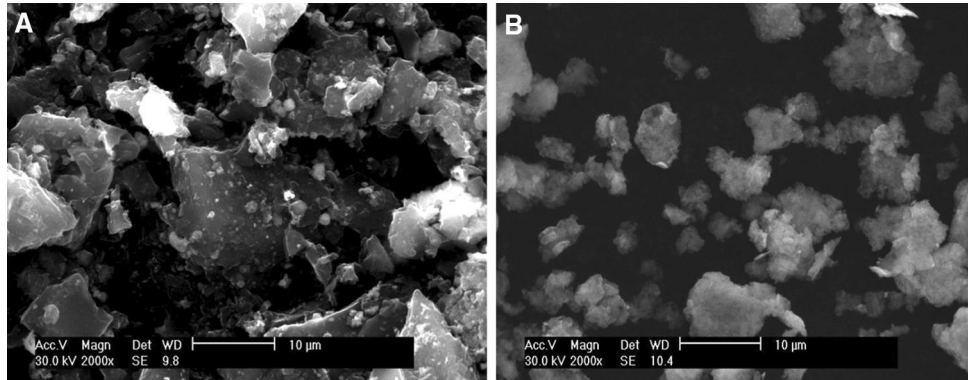
In this work, fresh ACCu–CoSPc and exhausted sample were examined by SEM–EDS. The shape and size of the adsorbent could substantially affect the adsorption capacity. As illustrated in Fig. 6a, numerous particles are spreading on the surface of adsorbent, which makes the surface of fresh catalyst obviously undulated. The size of particles seems to be unevenly distributed. As shown in Table 2, results from EDS analysis indicated that Cu and Co have been deposited on AC successfully. Subsequent XRD analysis suggested that Cu mainly exists in the form of  $\text{CuO}$  and  $\text{Cu}_2\text{O}$ . Compared with fresh sample, significant changes have occurred on the surface of exhausted



**Fig. 4**  $\text{N}_2$  adsorption isotherms of catalysts

**Table 1** Porous properties of AC samples

Samples	$S_{\text{BET}}$ ( $\text{m}^2/\text{g}$ )	$V_{\text{micro}}$ ( $\text{cm}^3/\text{g}$ )	$V_{\text{total}}$ ( $\text{cm}^3/\text{g}$ )	$D_{\text{average}}$ (nm)
AC	927.9	0.4528	0.4621	1.093
AC <sub>Cu–CoSPc</sub>	751.1	0.3902	0.3671	1.1096
AC <sub>Cu–CoSPc–CS<sub>2</sub></sub>	690.2	0.3237	0.3268	1.2083

**Fig. 6** SEM images of the surface of ACCu–CoSPc before (a) and after adsorption (b)**Table 2** EDS analysis of the surface of modified activated carbon

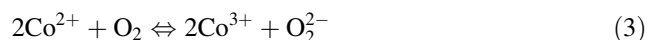
Sample	C	O	Al	Si	Ca	S	Co	Cu
AC								
wt%	88.04	9.10	0.80	0.95	1.11	0	0	0
at.%	92.32	6.53	0.37	0.43	0.035	0	0	0
AC <sub>Cu–CoSPc</sub>								
wt%	58.53	18.12	1.66	02.72	01.46	0.46	01.22	15.83
at.%	73.54	16.43	0.94	01.49	00.56	0.13	00.46	06.45
AC <sub>Cu–CoSPc–CS<sub>2</sub></sub>								
wt%	59.81	19.93	1.63	02.71	01.51	01.76	03.21	09.44
at.%	74.34	17.11	0.91	01.25	00.62	00.79	01.64	03.34

adsorbent (Fig. 6b). For instance, the gap is filled with crystals, the surface became smooth, and the brightness decreased. EDS results in Table 2 displayed that, S content was significantly increased after adsorption. S content of ACCu–CoSPc–CS<sub>2</sub> sample increases to 1.76 %, whereas the S content of ACCu–CoSPc is 0.46 %. In other words, the modified carbon material has purifying effect on CS<sub>2</sub>. The sulfides and sulfur oxides generated can be adsorbed on the surface or inside the pore, thus they might cover the active sites of the adsorbent, diming the active ingredient and reducing adsorbent activity.

### 3.6 XRD analysis

The phase and crystalline orientation of ACCu–CoSPc have been determined by XRD analysis, as shown in Fig. 7. Specifically, Cu mainly exists as CuO (Nguyen–Thanh and Bandosz 2005) and Cu<sub>2</sub>O in the modified adsorbent, and the latter could be resulted from the shortened baking time for the preventing of ashing adsorbent.

The existence of CuO and Cu<sub>2</sub>O can also be proved in the later analysis of XPS. Co<sub>2</sub>O<sub>3</sub> and Co<sub>2</sub>SiO<sub>4</sub> are the dominant form of Co f in samples. The conversion between Co<sup>3+</sup> and Co<sup>2+</sup> seemed to play a role in the electron transfer process involved in the following oxidation reaction:



No diffraction peak concerns S can be observed in the XRD spectrogram, however, the EDS result can verify the existence of S in ACCu–CoSPc sample. Concern to the reason about this phenomenon, it might results from the low concentration and the high dispersion of CoSPc in adsorbent.

### 3.7 X-ray photoelectron spectroscopic analysis

XPS analysis was employed to evaluate the chemical states of elements in ACCu–CoSPc and ACCu–CoSPc–CS<sub>2</sub> samples. Figure 8 showed the XPS spectra of core level binding energies of Cu 2p (a) before adsorption, as well as

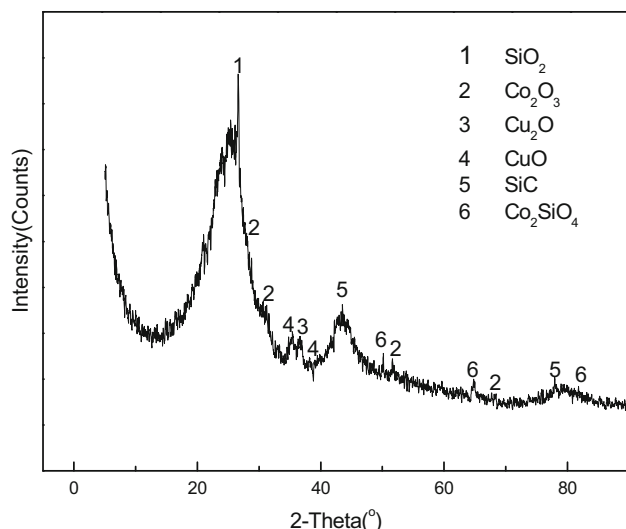


**Fig. 7** Representative XRD pattern of ACCu–CoSPc

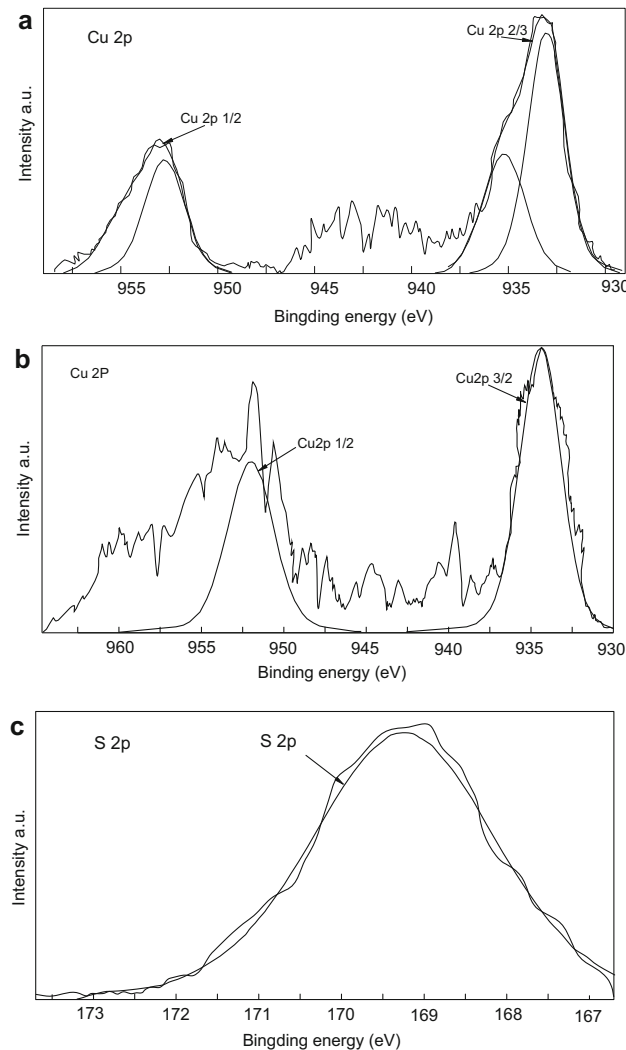


**Fig. 8** XPS spectra of ACCu–CoSPc for Cu 2p (a) and ACCu–CoSPc–CS<sub>2</sub> for Cu 2p (b) S 2p (c)

S 2p (c) and Cu 2p (b) after adsorption. Furthermore, Cu 2p<sub>3/2</sub> peaks locate within the range of 933–936 eV, which indicated that Cu primarily exists as CuO and Cu<sub>2</sub>O (Borgohain et al. 2000). This result was consistent with the XRD results illustrated in Fig. 7.

The XPS analysis for Cu 2p and S 2p of ACCu–CoSPc–CS<sub>2</sub> has also been conducted to identify reaction products. Figure 8 showed an S 2p peak centered around 169.27 eV, indicating the possible presence of SO<sub>4</sub><sup>2-</sup> (Berger et al. 1996). Possibly, S species appeared in ACCu–CoSPc–CS<sub>2</sub> could be formed via oxidative processes. Barely no sign of S specie can be observed in the freshly prepared ACCu–CoSPc adsorbent, whereas the adsorbent after adsorption clearly contained S species.

These results indicated that ACCu–CoSPc plays a very important role in the CS<sub>2</sub> adsorption process, in which CS<sub>2</sub> seems to be fixed on the surface of the AC. Compared with plain AC, there is no doubt that a higher quantity of SO<sub>4</sub><sup>2-</sup> has been formed in the carbon sample modified with ACCu–CoSPc. These results suggested that ACCu–CoSPc might participate in the catalytic oxidation involved in the CS<sub>2</sub> adsorption process.

### 3.8 CO<sub>2</sub>-TPD analysis

CO<sub>2</sub>-TPD can be used to study the basicity distribution of AC samples and conduct thermal regeneration experiments. The influence of regeneration frequency on breakthrough time and composition of desorption tail gas were examined during thermal regeneration, which could provide detailed information about the adsorption mechanism.

Figure 9 showed the TPD spectra with a heating rate of 10 K/min. Notably, one desorption peak was observed in the TPD spectra of AC, whereas the TPD spectra of ACCu–CoSPc showed two desorption peaks. In addition,

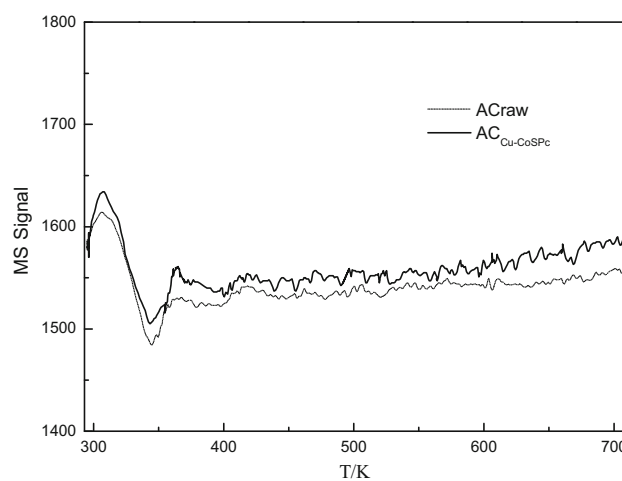


**Fig. 9** CO<sub>2</sub>-TPD profile of modified activated carbon

the peak area and temperature were different to each other (Shang et al. 1998a, b; West et al. 1998). It appears that the temperature of first desorption peak is low (about 310 K) for both AC and ACCu–CoSPc. However, the peak area of ACCu–CoSPc was found to be 32.39 % more than AC, indicating that the number of active centers in the former material should be increased, thus an enhanced adsorption capacity would be obtained. What's more, it can also be concluded that the basicity of adsorbent plays a positive role in CS<sub>2</sub> oxidation process.

### 3.9 Thermal regeneration

The composition of desorption tail gas were examined during the thermal regeneration process involving TPD. The relationship between the concentration of sulfur compound in off gas and desorption temperature was presented in Fig. 10. Specifically, SO<sub>2</sub>, CS<sub>2</sub> and COS are all detected in the effluent gas generated by ACCu–CoSPc–CS<sub>2</sub> during the TPD process. It is noteworthy that SO<sub>2</sub> and CS<sub>2</sub> are the primary sulfur compounds detected, accompanied with trace amount of COS. This result confirmed that the adsorption and oxidization of CS<sub>2</sub> occur on the surface of carbon, and part of CS<sub>2</sub> is adsorbed on the surface of adsorbent by physical adsorption, and another part of CS<sub>2</sub> is oxidized and then adsorbed on the adsorbent as SO<sub>2</sub> and COS.

TPD can also be used for the regeneration experiments of spent adsorbents. Figure 11 shows the CS<sub>2</sub> breakthrough behavior of ACCu–CoSPc adsorbent that was used in a CS<sub>2</sub> breakthrough test followed by TPD regeneration (sample named ACCu–CoSPc-R1, ACCu–CoSPc-R2, and ACCu–CoSPc-R3). Surprisingly, the adsorption behaviors of the spent adsorbents ACCu–CoSPc-R1 were found to be

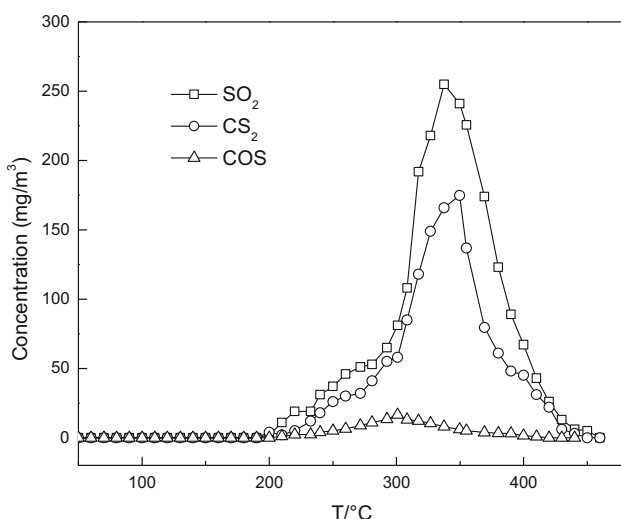


**Fig. 10** Desorption of ACCu–CoSPc–CS<sub>2</sub>

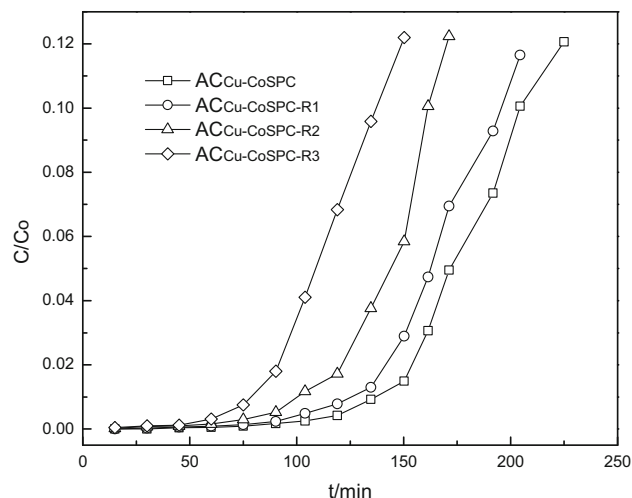
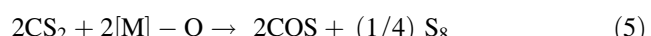
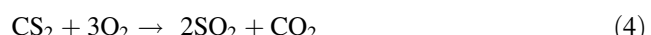


**Fig. 11** Influence of regeneration frequency of ACCu–CoSPc on breakthrough curve of CS<sub>2</sub>

similar to fresh ACCu–CoSPc. However, ACCu–CoSPc-R2 and ACCu–CoSPc-R3 displayed a shorter breakthrough time than ACCu–CoSPc-R1. Even the adsorption reaction has been lasted for 130 min, the purification efficiency of ACCu–CoSPc-R3 for CS<sub>2</sub> still remained above 90 %. This finding indicated that spent ACCu–CoSPc can be regenerated by thermal desorption for at least two times without detectable capacity loss.

Based on these results, we propose a plausible interaction mechanism between CS<sub>2</sub> and the surface of ACCu–CoSPc. Initially, the adsorbed CS<sub>2</sub> reacts with active oxygen generated by the active ingredient on the surface of modified carbon to produce active state sulfur and COS. Subsequently, part of the active sulfur compounds were converted to orthogonal  $\alpha$ -S<sub>8</sub> products, and the other part of the active sulfur is further oxidized to SO<sub>2</sub> and SO<sub>4</sub><sup>2-</sup>.

In summary, the macroscopic reaction can be represented as follows:



## 4 Conclusion

Five adsorbents have been prepared by impregnation method and their CS<sub>2</sub> adsorption capacities were evaluated. Comparing with other adsorbents, Cu and CoSPc modified AC showed a significant improvement on CS<sub>2</sub> adsorption with a breakthrough time of 210 min. In this case, the adsorption capacity of 13.35 mg CS<sub>2</sub>/g AC was obtained. By exploring different reaction conditions, the optimal reaction temperature was determined as 20 °C.

Based on the results obtained from spectral characterization, it can be concluded that Cu and CoSPc were favor of the formation of basic surface functional groups, which should significantly contribute to the significant increase of  $\text{CS}_2$  adsorption capacity. It is highly likely that Cu and CoSPc modified AC incorporated in micropores and worked as catalyst for the adsorption/oxidation process on the surface of impregnated sample.

After adsorption, sulfides and sulfur oxides generated are adsorbed on the surface or inside the pore, thus the active sites of adsorbent are covered, resulting in the reduction of adsorbent activity. The spent ACCu–CoSPc can be regenerated by thermal desorption for at least two times with less capacity loss.

**Acknowledgments** This work was supported by the National Natural Science Foundation of China (No. 51268021, U1137603), 863 National High-tech Development Plan Foundation (No. 2012AA062504).

## References

Allali, N., Marie, A.M., Danot, M., et al.: Carbon-supported and alumina-supported niobium sulfide catalysts. *J. Catal.* **156**, 279–289 (1995)

Bandosz, T.J.: Effect of pore structure and surface chemistry of virgin activated carbons on removal of hydrogen sulfide. *Carbon* **37**, 483–491 (1999)

Bandosz, T.J.: On the adsorption/oxidation of hydrogen sulfide on activated carbons at ambient temperatures. *J. Colloid Interface Sci.* **246**, 1–20 (2002)

Berger, F., Beche, E., Berjoan, R., et al.: An XPS and FTIR study of  $\text{SO}_2$  adsorption on  $\text{SnO}_2$  surfaces. *Appl. Surf. Sci.* **93**, 9–16 (1996)

Borgohain, K., Singh, J.B., Rao, M.V.R., et al.: Quantum size effects in  $\text{CuO}$  nanoparticles. *Phys. Rev. B* **61**, 11093 (2000)

Brasquet, C., Le Cloirec, P.: Adsorption onto activated carbon fibers: application to water and air treatments. *Carbon* **35**, 1307–1313 (1997)

Brunauer, S., Deming, L.S., Deming, W.E., et al.: On a theory of the vander waals adsorption of gases. *J. Am. Chem. Soc.* **62**, 1723–1732 (1940)

Cui, H., Turn, S.Q.: Adsorption/desorption of dimethylsulfide on activated carbon modified with iron chloride. *Appl. Catal. B. Environ.* **88**, 25–31 (2009)

Ghittori, S., Maestri, L., Contardi, I.: Biological monitoring of workers exposed to carbon disulfide ( $\text{CS}_2$ ) in a viscose rayon fibers factory. *Am. J. Ind. Med.* **33**, 87–478 (1998)

Liu, H.C., Yang, X.Y., Ran, G.P., et al.: Basic calcined Mg-Al hydrotalcite supported cobaltphthalocyanines catalysts for mercaptan autoxidation. *Petrochem. Technol.* **29**, 742–745 (2000)

Mei, H., Hu, M., Ma, H.X., et al.: Preparation and characterization of  $\text{NiO}/\text{MgO}/\text{Al}_2\text{O}_3$  supported CoPcS catalyst and its application to mercaptan oxidation. *Fuel Process. Technol.* **88**, 343–348 (2007)

Nguyen-Thanh, D., Bandosz, T.J.: Activated carbons with metal containing bentonite binders as adsorbents of hydrogen sulfide. *Carbon* **43**, 359–367 (2005)

Ning, P., Wang, X.Y., Hans, J.B., et al.: Removal of phosphorus and sulfur from yellow phosphorus off-gas by metal-modified activated carbon. *Clean Prod.* **19**, 1547–1552 (2011)

Oliver, T.M., Jugoslav, K., Aleksandar, P., et al.: Synthetic activated carbons for the removal of hydrogen cyanide from air. *Chem. Eng. Process.* **44**, 1181–1187 (2005)

Planeix, J.M., Coustel, N., Coq, B., et al.: Application of carbon nanotubes as supports in heterogeneous catalysis. *J. Am. Chem. Soc.* **116**, 7935–7936 (1994)

Shang, G.J., Li, C.H., Guo, H.X.: Hydrolysis of carbon sulfide and carbon disulfide over alumina based catalysis II. Study on  $\text{CO}_2$ -TPD of catalysis. *J. Nat. Gas Chem.* **7**, 24–30 (1998a)

Shang, G.J., Li, C.H., Guo, H.X.: Hydrolysis of carbonyl sulfide and carbon disulfide over alumina based catalysis I. Study on activities of COS and  $\text{CS}_2$  hydrolysis. *J. Nat. Gas Chem.* **7**, 16–23 (1998b)

Tong, S., Dalla, L.I.G., Chuang, K.T.: Appraisal of catalysts for the hydrolysis of carbon disulfide. *Can. J. Chem. Eng.* **70**, 516–522 (1992)

Wang, H., Yi, H., Tang, X., et al.: Reactivation of CoNiAl calcined hydrotalcite-like compounds for hydrolysis of carbonyl sulfide. *Ind. Eng. Chem. Res.* **52**, 9331–9336 (2013)

Wang, L., Wang, S., Yuan, Q.: Removal of carbon disulfide via coupled reactions on a bi-functional catalyst: experimental and modeling results. *Chemosphere* **69**, 1689–1694 (2007)

West, J., Williams, B.P., Young, N.C., et al.: New directions for COS hydrolysis: low temperature alumina catalysis. *Stud. Surf. Sci. Catal.* **119**, 373–378 (1998)

Williams, B.P., Nicola, C., Young, J.W.: Carbonyl sulphide hydrolysis using alumina catalysts. *Catal. Today* **49**, 99–104 (1999)

Yang, J., Juan, P., Shen, Z.M., et al.: Removal of carbon disulfide ( $\text{CS}_2$ ) from water via adsorption on active carbon fiber (ACF). *Carbon* **44**, 1367–1375 (2006)

Zhao, X., Yue, Y., Zhang, Y., et al.: Mesoporous alumina molecular sieves: characterization and catalytic activity in hydrolysis of carbon disulfide. *Catal. Lett.* **89**, 41–47 (2003)